

The development of near-vent volcanic ash cloud layers due to inhomogeneous atmospheric turbulence and relationship to wind shear

Marcus Bursik ^{1,*}ORCID: 0000-0002-9312-5202, Qingyuan Yang ²

Adele Bear-Crozier ³, Michael Pavolonis ⁴ and Andrew Tupper ³

¹ Center for Geohazards Studies,

University at Buffalo, Buffalo NY USA

² Earth Observatory of Singapore,

Nanyang Technological University, Singapore

³ Bureau of Meteorology, Melbourne, Australia

⁴ NOAA Cooperative Institute for

Meteorological Satellite Studies University of Wisconsin, Madison WI USA

Correspondence: mib@buffalo.edu; Tel.: +1-716-645-4265

January 7, 2021

Abstract

Volcanic ash clouds often become multilayered and thin with distance from the vent. We explore one mechanism for development of this layered structure. We review data on the characteristics of turbulence layering in the free atmosphere, as well as examples of observations of layered clouds both near-vent and distally. We then explore and contrast the output of volcanic ash transport and dispersal models with models that explicitly use the observed layered structure of atmospheric turbulence. The results suggest that the alternation of turbulent and quiescent atmospheric layers provides one mechanism for development of multilayered ash clouds by modulating the manner in which settling occurs.

Keywords: ash cloud; volcanic cloud; Pinatubo

1 Introduction

Volcanic ash is a multi-billion dollar economic hazard to aviation, as shown during the 2010 eruptions of Eyjafjalla-jökull, Iceland [Casadevall, 1994; Mazzocchi et al., 2010]. It is also a risk to flight safety, with hundreds of encounters of varying severity recorded, and several instances of multiple engine flame-out in flight. The International Airways

Volcano Watch (IAVW), which seeks to safely separate aircraft from volcanic ash in flight, relies on detecting areas of ash and forecasting its future movement [Tupper *et al.*, 2007]. However, the forecasting of ash presence and concentration is generally poorly resolved vertically, although there is some progress in this direction, e.g., [Heinold *et al.*, 2012; Kristiansen *et al.*, 2015]. Aircraft flying in a supposedly ash-contaminated region at a particular altitude may encounter no ash or significant and potentially damaging amounts, due to the high degree of ash stratification with altitude. The improved understanding and forecasting of stratification would assist enormously in managing the hazard and support the continuing development of the IAVW.

Photography and satellite imagery of numerous volcanic eruptions show that stratification or layering of volcanic clouds is a fundamental aspect of volcanic cloud development (Fig. 1). Lidar backscatter data have been key in defining this layered structure in distal regions (Fig. 2). Volcanic layers can be stratospheric as well as tropospheric.

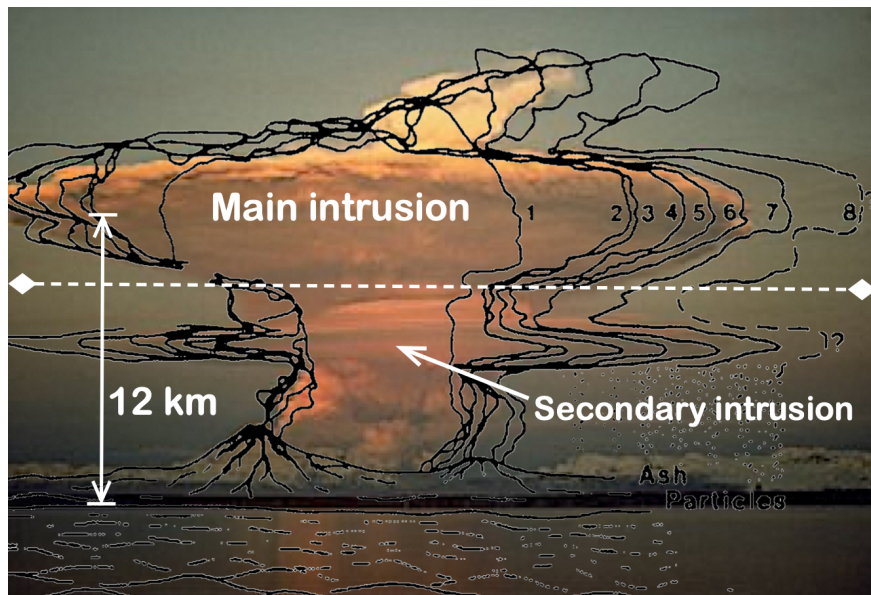


Figure 1: Photograph and tracing of eruption of Redoubt volcano, AK, 21 Apr 1990, showing plume overshoot, main umbrella intrusion and particle rich secondary intrusion. Tracings show growth of cloud layers through different time steps (numbered solid lines), long dashed where partly obscured. White dashed line, tropopause. Modified from *Woods and Kienle* [1994]

The layers form and separate by numerous processes, some unique to volcanic clouds. The primary volcanic cloud layer near the vent, such as the volcanic umbrella cloud or anvil cloud, arises from the driving of hot eruptive gas and ash parcels outward around their equilibrium level, or neutral buoyancy height [Sparks *et al.*, 1997]. Ash accretion, ash re-entrainment, source variability – injection of ash at different altitudes with changing eruption rate and wind fields, and gas-ash separation cause development of multiple layers [Holasek *et al.*, 1996a; Tupper *et al.*, 2004; Thorsteinsson *et al.*, 2012]. Double diffusion and convective sediment flux to a single [Woods and Kienle, 1994; Bursik, 1998; Hoyal *et al.*, 1999a, b; Carazzo and Jellinek, 2012] and multiple [Carazzo and Jellinek, 2013] levels by descending fingers that intrude below the level of a major volcanic cloud layer have been observed, and recreated in the laboratory. As suggested by brightness temperatures over the surface of near-vent clouds and ground

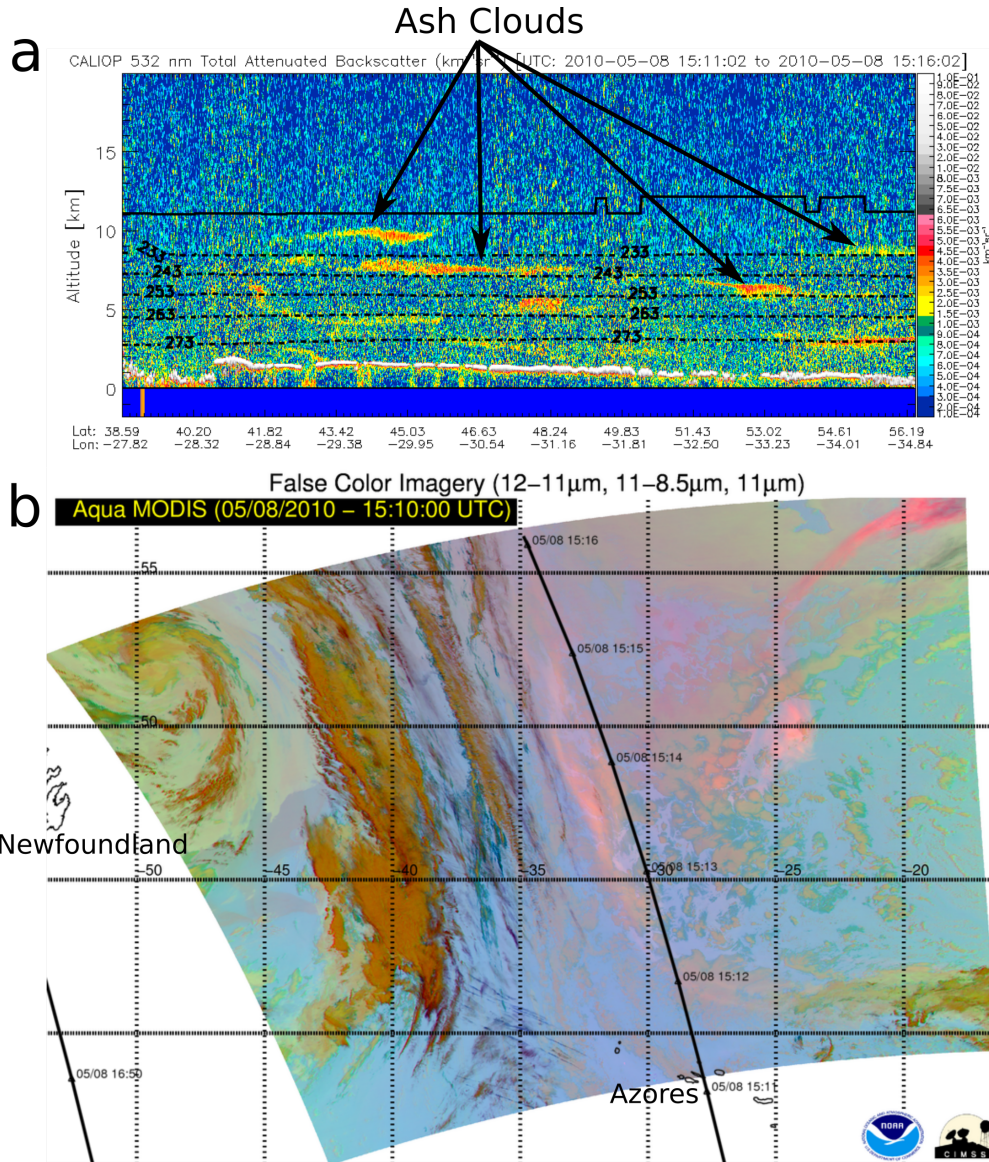


Figure 2: **(a)** CALIOP nadir LIDAR total attenuated backscatter (along track shown in **(b)**) showing complex layering of Eyjafjallajökull ash cloud on 8 May, 2010, isotherms (kelvins, black dotted lines) and tropopause (black solid line). **(b)** Aqua-MODIS RGB false color image [Pavolonis *et al.*, 2013] of North Atlantic capturing this ash cloud (pink hues).

based photography, umbrella clouds can be solitary, accompanied by a single lower intrusion resulting from re-entrainment and column-edge downflow [Woods and Kienle, 1994; Bursik, 1998] or accompanied by lower level skirt clouds [Barr, 1982], which may or may not contain ash. Mechanical unmixing of particulate-laden and gaseous volcanic cloud components has been noted as a further cause of volcanic layer formation [Holasek *et al.*, 1996b; Fero *et al.*, 2009], perhaps enhanced by gravity current slumping of the particle laden component [Prata *et al.*, 2017].

In contrast to the well-defined and complex layers discussed above, volcanic ash transport and dispersal models (VATDs), used to forecast ash cloud motion, display

layering of only a single ash cloud, if derived from wind shear; or after the fact from a numerical inversion for variable source height, which is otherwise assumed a fixed parameter ([*Kristiansen et al.*, 2015]). Although horizontal, planview resolution can be good, VATDs thus have difficulty in reproducing the vertical thickness and multilayering of distal volcanic clouds [*Devenish et al.*, 2012; *Folch et al.*, 2012; *Heinold et al.*, 2012]. In VATDs, dispersal in the vertical direction is commonly described by a single vertical diffusivity, κ_z , which in many models is taken to have the same value as the horizontal diffusivity, κ_h ; the result is then uniform or isotropic ash dispersion.

1.1 Problem Statement

The formation mechanism and morphology of distal ash cloud layers are poorly understood, and one potential mechanism for their formation and characteristics is the subject of the present contribution. Our working hypothesis is that, with particle settling, the structure of the atmosphere itself can cause layer formation, through the process of enhanced suspension in vertically restricted regions of high turbulence. Given that the mechanism explored herein results from the properties of the atmosphere itself, it may be the primary, distal layer-forming mechanism. Understanding the reason for the occurrence and morphology of specific ash-rich cloud layers is critical for correctly characterizing extended persistence of ash in the atmosphere, especially when multiple separate layers occur together. Satellite sensors penetrate only partially into the highest layer of an optically thick cloud, and satellite remote sensing algorithms are most sensitive to the column integrated ash properties, when multiple optically thin layers are present. A correct understanding of layer formation and morphology is also critical for any attempts to construct VATD models capable of producing output consistent with observations of vertical dispersion.

2 Materials and Methods

2.1 Background Data

2.1.1 Atmosphere

Volcanic clouds both create turbulence and are subject to ambient atmospheric turbulence. In volcanic clouds near the vent, turbulence is created by both the Rayleigh-Taylor and Kelvin-Helmholtz mechanisms, as the clouds intrude into the atmosphere as gravity currents. Kelvin-Helmholtz instability is driven by the shear between the intruding cloud and the atmosphere [*Britter and Simpson*, 1981]. Rayleigh-Taylor instability is driven by convective sedimentation, fingering and local, eddy scale density reversal [*Woods and Kienle*, 1994; *Holasek et al.*, 1996b; *Chakraborty et al.*, 2006].

Information of sufficient resolution in the vertical direction to discover and characterize the layered structure of the atmosphere is obtained from airborne measurement campaigns or rawinsonde balloon releases [*Dehghan et al.*, 2014; *Cho et al.*, 2003; *Pavelin et al.*, 2002]. Several methods have been developed to derive turbulence from rawinsonde and other high-resolution data. *Vasseur and Vanhoenacker* [1998] measured changes in the refractive index structure parameter for radio waves, as turbulence causes changes in the refractive index, based on rawinsonde pressure, temperature, humidity, wind speed and wind direction data. *Clayson and Kantha* [2008] used

variations in the potential temperature profile from an idealized profile to calculate the Thorpe scale, and derive turbulent dissipation and diffusivity. These estimates can be made for single rawinsonde profiles with simple calculations. There are drawbacks of course to extrapolating such high-resolution or point data to a regional scale because of spatial and temporal inhomogeneity; the troposphere is highly transient and spatially variable [Clayson and Kantha, 2008; Thouret et al., 2000]. Tropospheric isobaric surfaces are not necessarily parallel to the earth’s surface, especially at fronts and in mountain waves Sharman et al. [2012]. Fronts are associated with tropopause folds, non-horizontal isobaric surfaces separating cold from warm air, and turbulence in folds is generated by local dynamic and convective instabilities. Mountain waves form as the density stratified atmosphere flows past the lee side of a mountain or mountain range. These waves can break, resulting in local turbulence concentrated in non-horizontal layers.

In the free atmosphere, parameters such as moisture content and temperature do not change monotonically with height; there are regions of relatively homogeneous, convecting or turbulent air, separated by regions in which parameters vary rapidly [Vasseur and Vanhoenacker, 1998; Sharman et al., 2012]. Both the stratosphere and the troposphere are layered on scales of $\mathcal{O}[0.1 - 1\text{km}]$ [Maekawa et al., 1993; Wilson et al., 2014], but the layers in the troposphere tend to be more transient and discontinuous [Gage et al., 1980]. In the troposphere, layers of high turbulence, including high vertical turbulence, can be indicated by constant relative humidity (RH) or mixing ratio, q [Cho et al., 2003]. RH is thus an important proxy for turbulence intensity. (Atmospheric moisture is also important in aiding plume lift, especially in plumes from weak sources, or at low latitude, where the moisture content is high [Sparks et al., 1997; Tupper et al., 2009]). As a result of the layering, large-volume or bulk turbulence is highly anisotropic ($\kappa_h \gg \kappa_z$), and only within thin, well-defined layers is it approximately isotropic ($\kappa_{h,local} \approx \kappa_{z,local}$) [Gage et al., 1980].

2.1.2 Ash Clouds

Data are available from a number of sources on the shape and structure of both near-vent and distal ash clouds. In the near-vent region, data tend to be more limited, due to the greater optical depth. Nevertheless, cloud brightness temperature (BT) as measured from nadir-looking geostationary and low-earth orbiting satellites provides much useful information, as the topography of the top of the near-vent clouds can be quite variable, with a distinct high point or swell above the central vent that might be many kilometers above the top of the main umbrella cloud [Fero et al., 2009]. In addition, airborne and ground-based photography and videography have provided extensive data on the features at the base of the main umbrella or anvil, and within the underlying cloud layers. Visible satellite imaging of the near vent cloud top consistently reveals strong, well-defined three-dimensional vortex structures above the vent, which evolve to smooth, somewhat more diffuse structures in the umbrella cloud [Pouget et al., 2016].

Although the air can be choked with opaque, diffuse ash bodies that extend to ground level near vent (Fig. 3a, b), and although gravitational intrusions, such as umbrella clouds, are wedge-shaped by nature and therefore of variable depth (Fig. 3c), measurements have been made of the ΔBT between cloud top and edge of the main cloud. The results suggest that umbrella clouds at the vent typically encompass depths

of $\mathcal{O}[5]$ km (Fig. 1; Table 1), which makes a large mass of ash available for transport at sometimes high levels. Some of the lower near-vent clouds also become distal clouds (Fig. 3d). In some cases, therefore, it might be possible to find the entire troposphere and even lower stratosphere charged with ash, or only a distinct layer or two of $\mathcal{O}[5]$ km depth.

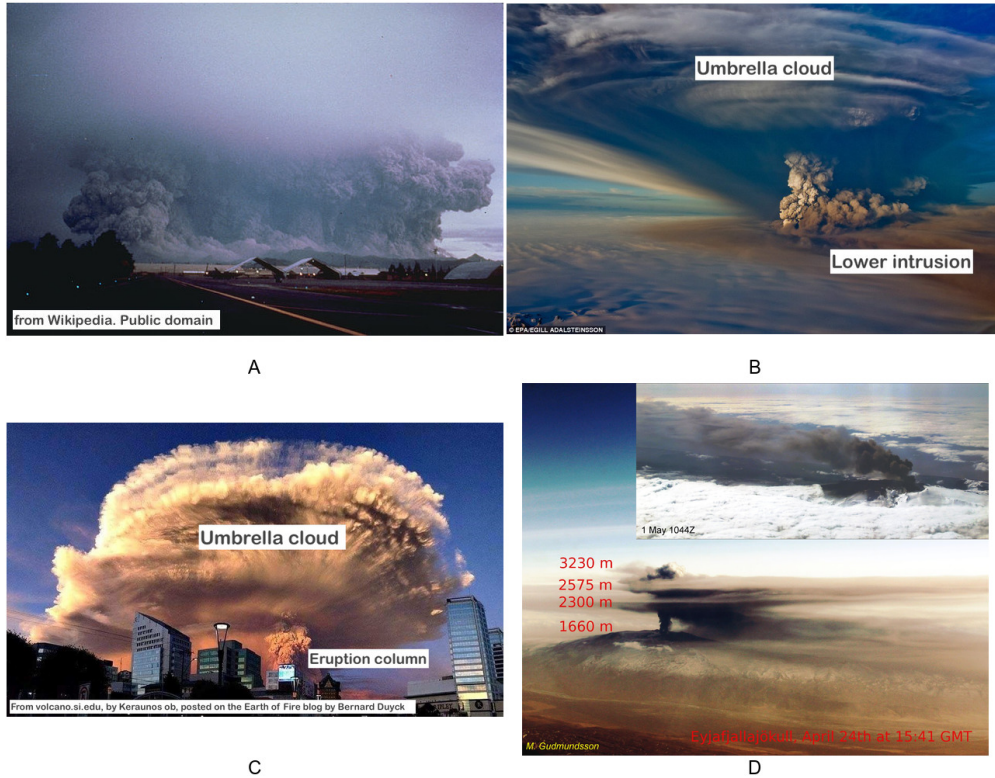


Figure 3: (a) Eruption of Pinatubo, June 15, 1991. Emission from vent as well as pyroclastic flows results in ash injecting into the atmosphere at all heights up to 40 km. In the public domain. (b) Eruption of Grimsvotn, May 22, 2011. Ash injected in umbrella cloud (above), and in lower intrusion from secondary, ash-rich cloud (below). Umbrella at 18-20 km. Modified from <https://www.dailymail.co.uk/news/article-1389846/Iceland-volcano-eruption-2011-Grimsvotn-hurles-ash-plume-12-miles-sky.html>. (c) Eruption of Calbuco, April 22, 2015. Ash injected in single umbrella cloud at c. 15 km. Modified from <https://volcano.si.edu/volcano.cfm?vn=358020>. (d) Eruption of Eyjafjallajökull, April 24 and May 1, 2010. Ash injected at multiple heights in relatively quiescent atmosphere on April 24. On May 1, under windy conditions, ash mostly injected from single downwind plume. Modified from photographs by M. Gudmundsson.

In the distal region, airborne lidar, EARLINET-AERONET and CALIOP data typically show much thinner, more discontinuous cloud structures (Fig. 2). Three separate tabulations of distal ash cloud layer data for the Eyjafjallajökull plume have been published [Jonsson *et al.*, 1996; Ansmann *et al.*, 2011; Winker *et al.*, 2012]. These data suggest that distal clouds from this tropospheric eruption were typically 0.3-3 km thick, made up of 2-3 layers, with individual layers of 0.3-1.4 km depth, and maximum age of 129 h (\approx 1 week) (Table 2). Vernier *et al.* [2013] using CALIOP data, discerned

Table 1: Measured main, near-vent, upper volcanic cloud depth from top to cloud edge. Measured from geostationary imagery in first scene after eruption start (photography for Redoubt). Data from *Bear-Crozier et al.* [2020]; and *Pouget et al.* [2013] and *Holasek et al.* [1996a] (below divider)

Volcano	Eruption start date	Height, km ASL	Depth, km	No. layers
Tinakula	Oct 20, 2017, 2350 UT	16.6	4.9	1
Tinakula	Oct 20, 2017, 1930 UT	15.1	3.4	1
Rinjani	Aug 1, 2016, 0345 UT	5.5	4.0	1
Manam	Jul 31, 2015, 0132 UT	13.7	9.2†	2
Sangeang Api	May 11, 2014, 0832 UT	15.4	12.0†	2
Kelud	Feb 13, 2014, 1632 UT	15.3	2.8	1
Manam	Jan 27, 2005, 1400 UT	24.0	3.0	1
Manam	Oct 24, 2004, 2325 UT	18.5	1.5	1
Pinatubo	Jun 15, 1991, 2241 UT	23.6	4.7	1
Redoubt	Apr 21, 1990, 1412 UT	12.0	4.9	2
Mount Helens	St. May 18, 1980, 2020 UT	13.0	1.0	1

† Depth possibly overestimated.

two or more well-defined layers in the cloud from Puyehue-Cordon Caulle three weeks after the eruption. Some of the layers showed fold or wrap-around structures (Figure 1a in *Vernier et al.* [2013]), perhaps related to vertical-plane chaotic mixing [*Pierce and Fairlie*, 1993]. Clouds were up to 3 km thick, with individual layers of 0.1-2 km depth, in the upper troposphere-lower stratosphere (UTLS), centered on the tropopause at 8-14 km altitude. On July 12-13, 1991, 26 days after the last major eruption of Pinatubo, a lidar flight noted numerous stratospheric layers [*Winker and Osborn*, 1992]. The data showed a number of well-defined layers of 0.5-1 km depth between about 14 and 25 km altitude (Figure 1 in *Winker and Osborn* [1992]). Along much of the line of flight there were two layers, but in places there were up to five. In all studies cited above, distal ash layers were horizontal or tilted relative to the horizon, and had extents in the cross-transport direction of hundreds of km in the troposphere (Eyjafjallajökull), to thousands of km in the stratosphere (Puyehue, Pinatubo). Ash is retained longer in the stratosphere than in the troposphere as suggested by the data cited herein.

Once the particles have propagated far from vent (≈ 11 hr in the case of a large eruption, e.g., Pinatubo), they no longer retain significant memory of source conditions [*Fero et al.*, 2009]. Back trajectories of distal ash clouds for Eyjafjallajökull and Puyehue-Cordon Caullé are generally consistent with theoretically possible cloud heights at the source [*Winker et al.*, 2012; *Vernier et al.*, 2013]. However, it is not clear that ash was injected at these altitudes at the source, given uncertainties in vertical parcel motion and settling speed, or lack of incorporation thereof in the models [*Madankan et al.*, 2014; *Vernier et al.*, 2013]. It is at least possible that some cloud layers were generated at distance from the volcanic source.

The data presented herein, in text, Figures 2, 3, and Tables 1, 2, suggest that the number of layers increases with time, and the depth decreases (see also *Dacre et al.* [2015]). Volcanic source conditions are eventually lost after an eruption, meaning

Table 2: Measured distal Eyjafjallajökull cloud depths from CALIOP lidar. Data from *Winker et al.* [2012] (top), *Marenco et al.* [2011] (middle) and *Schumann et al.* [2011] (lower section). Note that number of layers varies with spatial position.

Date	Cloud	Height range km ASL	Depth km	Age, hr	No. lay- ers
Apr 15	20100415	1.41 – 3.23	0.51	< 6	–
Apr 16	20100416-a	3.77 – 5.50	0.58	30	> 1
Apr 16	20100416-b	1.97 – 7.27	0.67	24	> 1
Apr 17	20100417-a	0.20 – 6.28	0.76	42	1
Apr 17	20100417-b	0.05 – 4.00	0.61	42	1
Apr 18	20100418-a	3.14 – 5.59	0.81	66	–
Apr 18	20100418-b	3.75 – 6.49	0.86	66	–
Apr 19	20100419-a	3.20 – 5.26	1.06	71	–
Apr 19	20100419-c	2.48 – 3.94	0.45	30	–
Apr 19	20100419-d	4.63 – 5.20	0.41	114–126	–
Apr 20	20100420	0.05 – 1.88	1.08	20–24	–
May 4	20100504	2.3 – 5.5	0.5	–	1 – 2
May 5	20100505	2.4 – 4.5	0.9	–	1 – 2
May 14	20100514	5.1 – 8.1	1.1	–	1 – 3
May 16	20100516	3.4 – 5.5	1.2	–	1 – 3
May 17	20100517	3.5 – 5.6	1.3	–	1 – 3
May 18	20100518	2.5 – 4.9	0.9	–	1 – 3
Apr 19	20100419-1	3.9 – 5.6	1.7	105 – 111	> 1
Apr 19	20100419-2	3.5 – 3.8	0.3	104 – 108	1
Apr 19	20100419-3	3.9 – 4.2	0.3	105 – 108	1
Apr 22	20100422-4	0.7 – 5.5	–	49 – 50	diffuse
Apr 23	20100423-5	2.1 – 3.4	1.3	40 – 58	> 1
May 2	20100502-6	1.6 – 3.7	2.1	7.1 – 12	> 1
May 9	20100509-7	3.5 – 4.9	1.4	97 – 129	1
May 13	20100513-8	2.8 – 5.4	0.4 – 0.7	71 – 78	1 tilted
May 16	20100516-9	3.6 – 7.0	3.4	58 – 66	> 1
May 17	20100517-10	3.2 – 6.3	3.1	66 – 88	> 1
May 18	20100518-11	2.8 – 3.4	0.6	81 – 100	1
May 18	20100518-12	4.0 – 5.7	1.7	66 – 78	> 1

that the atmosphere completely controls cloud shape. Layers are more transient in the troposphere than in the stratosphere, as mentioned for certain eruptions (also, *cf.* data in Table 1 with 2; [*Thouret et al.*, 2000]). In summary, the features of volcanic clouds include the following:

1. Near-vent clouds often evolve from sharply defined with clear eddy or vortex structure to diffuse or diaphanous, into distal, thin well-defined layers with sharp, smooth boundaries
2. There are often multiple distal layers

3. Collocation in position in planview is common (stacking), but not pervasive
4. Sometimes distal cloud forms are horizontal; sometimes sloping or tilted relative to horizontal
5. Separate particle clouds exist, not only separate gas and ash clouds
6. Horizontal extent \gg vertical extent
7. Vertical extent of near-vent layers is $\mathcal{O}[5]$ km, which with time results in
8. Vertical extent of single, distal layers being $\mathcal{O}[0.1 - 1]$ km

The present contribution seeks to provide explanations for some of these features.

2.2 Model

The advection-diffusion equation forms the basis for all VATD models. To illustrate differences and potential problems in implementation of VATD and the underlying physics, in this section, we introduce two zeroth-order simplifications. Our goal is to contrast the basic behavior of an ash cloud under conditions of isotropic (or constant κ_h and κ_z) turbulence, as assumed in the models, and layered turbulence, as we find in the atmosphere. We base our modeling on generation of synthetic atmospheres with and without multiple turbulent layers separated by relatively quiescent air.

In the case of isotropic turbulence, we begin by assuming Cartesian coordinates, (x, y, z) , with velocity components, (u, v, w) . The three components of the turbulent diffusivity, $(\kappa_x, \kappa_y, \kappa_z)$ are the same, κ . The concentration of particles in the i -size fraction, C_i , varies in time, t and space as:

$$\frac{\partial C_i}{\partial t} + \frac{\partial}{\partial x} (uC_i) + \frac{\partial}{\partial y} (vC_i) + \frac{\partial}{\partial z} (wC_i) = \frac{\partial^2}{\partial x^2} (\kappa C_i) + \frac{\partial^2}{\partial y^2} (\kappa C_i) + \frac{\partial^2}{\partial z^2} (\kappa C_i) + \Phi \quad (1)$$

where Φ represents the source/sink function, which in the case of ash clouds is mostly represented by aggregation and disaggregation of small particles. In the present case, such processes are set to zero. We assume a two-dimensional system with a point-source in time and space, $w = w_s$, the settling speed, and that, following a streamtube, the motion of the volcanic cloud can be characterized by a single downwind coordinate direction s – for which the axis is everywhere tangent to the plume centerline, e.g., [Wright, 1977; Hopkins and Bridgman, 1985] – and speed U in that direction. Under these assumptions, the advection-diffusion equation becomes:

$$\frac{\partial C_i}{\partial t} + \frac{\partial}{\partial s} (UC_i) + \frac{\partial}{\partial z} (w_s C_i) = \frac{\partial^2}{\partial s^2} (\kappa C_i) + \frac{\partial^2}{\partial z^2} (\kappa C_i) \quad (2)$$

with the well-known solution for the impulse initial condition [Csanady, 1980; Roberts and Webster, 2002]:

$$C_i(s, z, t) = \frac{C_{i0}}{4\pi\kappa t} \exp \left[-\frac{(s - s_0 - Ut)^2 + (z - z_0 - w_s t)^2}{4\kappa t} \right]. \quad (3)$$

It is reasonably clear that the solution is a Gaussian in (s, z) , in which ash spreads, settles and is blown downwind with time.

In the second case, of layered turbulence, more realistic for the free atmosphere, we assume particles filling a layer of finite vertical extent. Due to its internal turbulence,

concentration varies in t but not in s or z within the layer, $C_i(s, z, t) = C_i(t)$. There is no flux at the upper boundary of such a layer, as any particles injected upwards by eddies will settle back down into the layer. There is a flux boundary condition at the lower boundary where $\kappa_z \rightarrow 0$, and in this case, the advection-diffusion equation becomes, at the lower boundary:

$$\frac{\partial}{\partial t}(C_i) + \frac{\partial}{\partial z}(w_s C_i) = 0 \quad (4)$$

If furthermore it can be assumed that some particles near the cloud base fall from the turbulent layer when their weight overcomes the internal turbulence at the lower cloud edge, thus developing a step-like concentration gradient at the base of the streamtube, then:

$$C_i(t, z) = H(z)C_i(t) \quad (5)$$

where $H(z)$ is the Heaviside step function, then:

$$\frac{\partial}{\partial t}(C_i) + \frac{\partial}{\partial z}(w_s C_i) = \frac{\partial C_i}{\partial t} + w_s C_i \frac{\partial H(z)}{\partial z} = 0 \quad (6)$$

Integrating through the layer depth, h :

$$\frac{\partial C_i}{\partial t} \int_0^h dz = -w_s C_i \int_0^h \delta(z) dz \quad (7)$$

we obtain:

$$\frac{dC_i}{dt} = -\frac{w_s}{h} C_i \quad (8)$$

which has solution:

$$C_i = C_{i0} \exp\left(-\frac{w_s(t - t_0)}{h}\right) \quad (9)$$

In the quiescent layer below the boundary, particles only settle and are advected downwind, there is no turbulence mechanism to enhance persistence within the layer. Thus, turbulent layers can retain particles longer than do quiescent layers because of continuing re-entrainment in eddies. Particles fall relatively rapidly through the quiescent layers because of uninhibited settling, sometimes even enhanced by the effects of convective sedimentation [*Hoyal et al.*, 1999a], which is not included in the present model.

Based on similarity theory, the timescales for the processes under the different particle transport conditions arising in different layers can be used to examine the conditions under which diffusion or settling dominates. From Eq 3, the timescale of vertical diffusion, τ_1 , through a layer of depth, h , is given as $\tau_1 = \frac{h^2}{\kappa}$. From Eq 9, the timescale of settling through the same layer, τ_2 , is $\tau_2 = \frac{h}{w_s}$. The ratio of the two timescales indicates domination of particle transport by settling or dispersion in the vertical direction. The ratio is given by the dimensionless group, Π_1 :

$$\Pi_1 = \frac{\tau_1}{\tau_2} = \frac{hw_s}{\kappa} \quad (10)$$

In the following section, we explore results from these simplifications and the similarity analysis, as well as numerical solutions to more complicated cases. Numerical solutions are provided for the Ash3D VATD model [*Schwaiger et al.*, 2012], as well as both Eulerian and Lagrangian model codes (Table 3).

3 Results

Following from Eq 3, spread from a point source in a VATD model, with isotropic turbulence and a wind of constant speed with height, is shown in Figure 4a, b. Ash diffuses and progressively spreads from the source as the center of mass descends at the settling speed. Using a higher settling speed, the rate at which the center of mass descends increases, but the rate at which the particles disperse from the center of mass remains constant. Thus, at any one height below the source, particles with a higher settling speed should be spread less distance from the source.

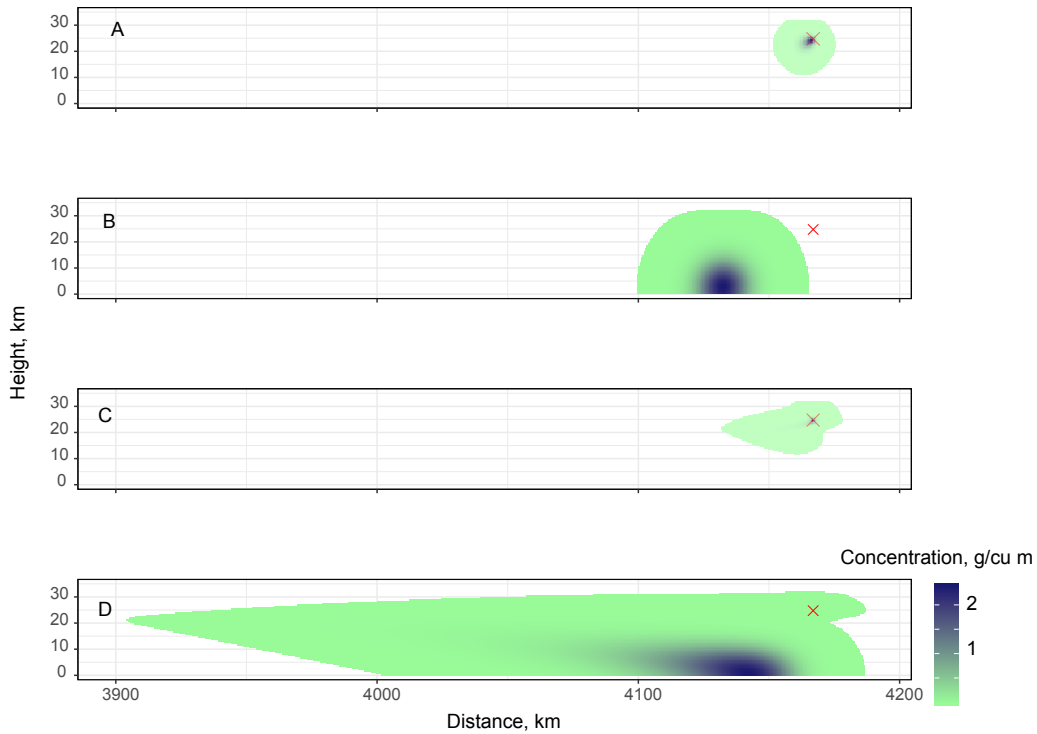


Figure 4: Cross sections through Ash3D output, with: **(a)** instantaneous source, showing advection, settling and isotropic dispersal of ash. 10 min after release. **(b)** instantaneous source, showing advection, settling and isotropic dispersal of ash. 120 min after release. **(c)** maintained source, showing advection with wind shear, settling under isotropic turbulence. 10 min after release. **(d)** maintained source, showing advection with wind shear, settling in isotropic turbulence. 120 min after release. Note that maintained source and wind shear result together in elongated dispersal pattern, and layer development. Red cross, source location.

Table 3: Simulation parameters. Duration refers to emission from vent.

Parameter	$\kappa = \text{const}$	$\kappa = \text{const}$	Layered sphere	Atmo-
	wind=const	windshear		
Simulation type	Ash3D	Ash3D	Lagrangian-1	Lagrangian-2
Source type	Point	Point	Point	Point
Source height, km	24.75	24.75	24.75	4.2
Particle size, μm	1000	1000	1000	40
Settling speed, m/s	3	3	3	0.02
Amount	0.01 km ³	0.01 km ³	1000 parcels	1000 parcels
Duration	0.2 hr	0.2 hr	Instantaneous	Instantaneous
Turbulent heights	–	–	24 – 25, 14.5 – 19 km	3.8 – 4.2, 2 –
Wind speed	5 m/s all elev	Below 19.75 km: 0 m/s 19.75 to 21.75 km: 10 m/s increasing to 50 m/s 21.75 to 23.75 km: 50 m/s decreasing to 10 m/s Above 23.75 km: 10 m/s	5 m/s	2.7 km 10 m/s 0 m/s
				3.8 – 4.2, 2 – 2.7 km 0 m/s

Dispersion in the presence of wind shear is shown in Figure 4c, d. The shear distorts the dispersal pattern from the idealized, spherically symmetric pattern seen in the constant wind field, causing an elongation in the dispersal pattern centered at the wind speed maximum. Because the deformation is by simple shear, cloud thinning does not occur. Wind-shear produced elongation thus creates a volcanic cloud layer that continues to deepen by diffusion.

In a layered atmosphere, we refer to Eq 10 to explore asymptotic behavior. In layers for which $\Pi_1 > 1$, the diffusivity is low relative to the settling speed, the timescale of diffusion is therefore long, hence motion is controlled by settling. In layers for which $\Pi_1 < 1$, the diffusivity is high relative to the settling speed, the timescale of settling is long, hence motion is dominated by diffusion. Note also that as h increases, the timescale of diffusion increases faster than does that for settling, meaning it becomes more likely the particles will exit a layer by settling than by diffusion. For a typical diffusivity of $\kappa = 1 \text{ m}^2/\text{s}$ in the UTLS [Wilson, 2004] at 10 km altitude, and layer of depth $h = 1 \text{ km}$, the critical settling speed, $w_{s,crit}$, dividing settling from diffusion dominated motion is c. 1 m/s, which would correspond to a pumice particle of diameter c. 100 μm at about 2400 kg/cu m (e.g., [Scollo et al., 2005]).

Results for a simple layered system are shown in Figures 5 and 6. These figures are simplified from the observations of Cho et al. [2003], who point out two layers of especially striking turbulence from 2-2.7 km and 3.8-4.2 km (Fig. 5a), but do not give specific values for turbulence intensity in any layers. We therefore apply turbulence in these two layers through a Lagrangian random walk, and in other layers, no turbulence. Particles in the turbulent layers, then, initiate the random walk, being “stuck” within the eddies of the turbulent layer (Fig. 5b). Consider the lower boundary of a layer with strong turbulence. All the particles there are subject to a random walk. They have a 50% percent probability of going up, and a 50% probability of going down. Those particles sent above the lower boundary due to turbulence are sent to a position higher above the boundary than their original position at the boundary. This will give them a greater chance to spend a longer time in the turbulent layer, whether or not one considers settling. Thus, for those layers dominated by the random walk and dispersion, $\Pi_1 < 1$, Eq 9 holds, and the behavior seen in Figures 5 (purple layers) and 6 (red and blue lines) occurs. Particles accumulate in the lowermost turbulent layers (e.g., blue curve in Figure 6), and once reaching a peak, settle out only slowly. Thus, the lower, turbulent layers are the most likely ones in which to observe particles on longer timescales.

The two modes of behavior, isotropic diffusion and layered diffusion, contrast starkly, as seen in explicitly comparing VATD output with that from the Lagrangian-1 model (Table 3; Fig. 7). Isotropic diffusion alone cannot lead to generation of ash layers away from source, but layered diffusion can, even in a constant windfield.

4 Discussion and Conclusions

In the present work, we have presented data and models on near-vent and distal volcanic cloud morphology and loading. We have performed numerical experiments comparing dispersal in an atmosphere with constant κ and wind, constant κ and wind shear, and variable κ_z with height. The observational data suggest that more distal clouds of depth $\mathcal{O}[0.1 \text{ to } 1] \text{ km}$ develop from near-vent clouds of depth generally 1 – 5 km. The

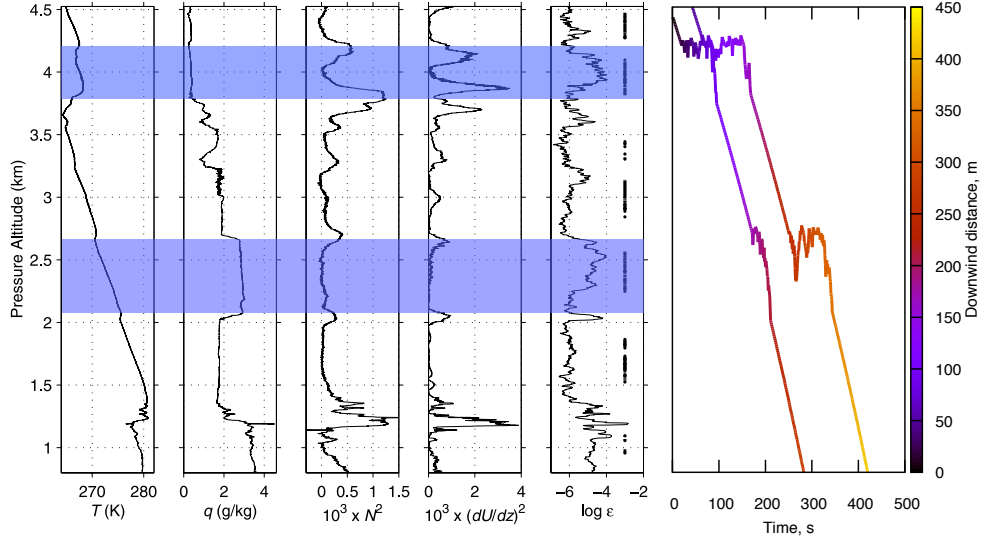


Figure 5: **(a)** Turbulent tropospheric layers (shaded) indicated by constant mixing ratio (q), high turbulent energy dissipation rate ($\log \varepsilon$), and bounded by high shear ($(dU/dz)^2$). Modified from *Cho et al.* [2003]. Shaded layers are used in simplified layer models Lagrangian-2 and Eulerian (Table 3) **(b)** Lagrangian paths of two volcanic particles settling through the turbulent layers, in which suspension is enhanced. This is output from model Lagrangian-2.

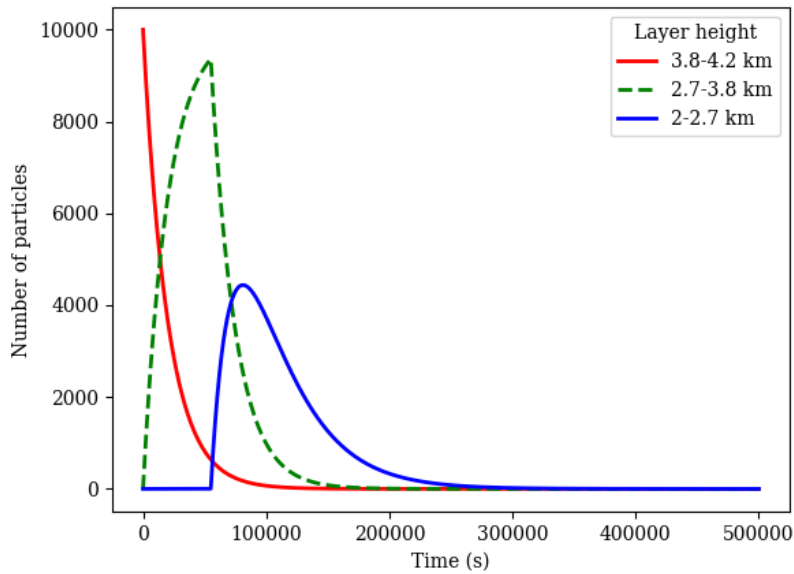


Figure 6: Eulerian model (Table 3) of number of particles in layered atmosphere. Middle layer is not turbulent (green dashed curve); upper and lower layers are turbulent (red and blue solid curves)

downwind clouds occur at heights consistent with the original eruption column heights for both tropospheric and stratospheric eruptions. The depth range of the distal layers,

being markedly less than the near-vent depth range, and the common stacking of more distal ash cloud layers, suggest that their development is controlled by atmospheric processes. The observations are consistent with the working hypothesis that the layering of the atmosphere in turbulence intensity, causing alternating suspension and settling dominated behavior of particles, is a cause of distal layer morphology.

The present model outputs (Figs. 4, 7) are consistent with those of VATD and backtrajectory models that layers can be produced under conditions of certain source characteristics or wind shear [Devenish *et al.*, 2012; Folch *et al.*, 2012; Heinold *et al.*, 2012; Winker *et al.*, 2012; Vernier *et al.*, 2013]. The model outputs assuming the atmosphere has multiple turbulent layers support the working hypothesis regarding the effects of an atmosphere layered with respect to turbulence intensity. Thus, in addition to the near-vent, volcanic and sedimentation processes causing formation of volcanic layers, processes associated with atmospheric layered turbulence also produce layering in ash clouds. These are often multilayered due to multiple, alternating layers of turbulent and quiescent air. The distal ash layers furthermore scale to the depth of the alternating turbulent and quiescent layers in the atmosphere, which are $\mathcal{O}[0.1 - 5]$ km deep.

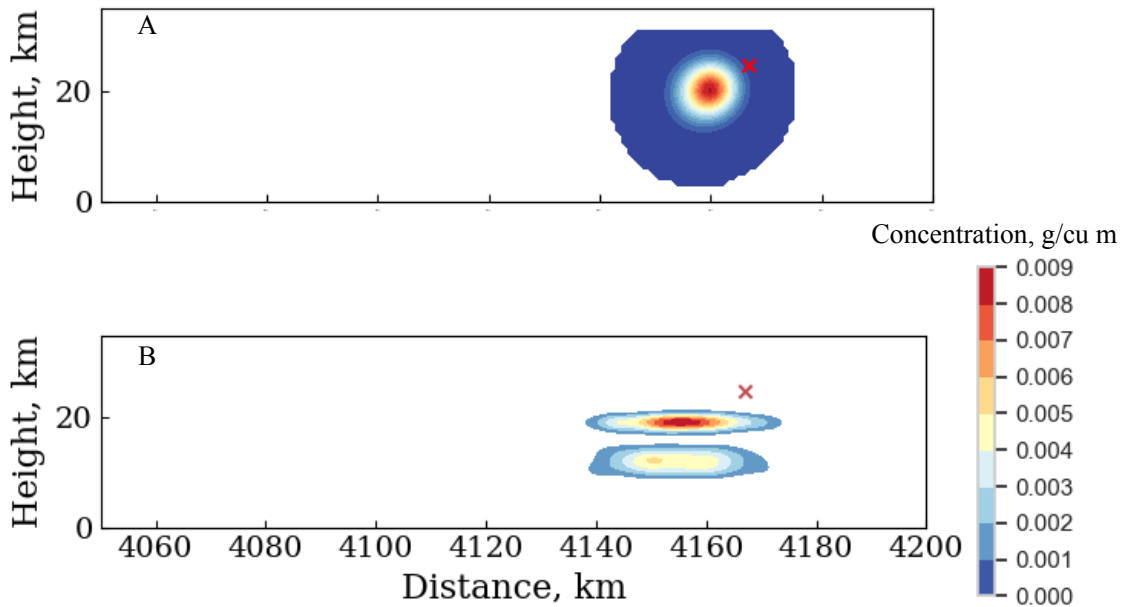


Figure 7: **(a)** Cross section through Ash3D output (Table 3), with instantaneous source and no wind shear, showing advection, settling and isotropic dispersal of ash. **(b)** Cross section through Lagrangian-1 dispersion model (Table 3 with turbulence layered atmosphere, showing advection, settling and non-isotropic ash dispersal. Red \times is point of origin for particles, and color gradient is scaled to concentration in both.

Because of the alternating turbulent and quiescent structure in the troposphere and stratosphere, volcanic ash clouds tend to separate vertically over time, leading to them the distinct layering or banded appearance in imagery. The turbulent layers retain particles longer than the quiescent layers because the turbulence retains particles in suspension. Particles fall more rapidly through the relatively quiescent layers (lower κ_z) by single particle settling, or because of convective sedimentation.

The results suggest that to better model the position and morphology of ash clouds for aviation safety and other purposes in VATDs, the vertical characteristics of the atmosphere need to be better resolved than is typical at present. Because of the importance of turbulence and moisture to layer formation, it is critical that these two parameters especially be estimated well, and at as high a vertical resolution as possible.

Abbreviations. The following abbreviations are used in this manuscript:

AERONET	AERosol RObotic NETwork
BT	Brightness Temperature
CALIOP	Cloud-Aerosol Lidar with Orthogonal Polarization
EARLINET	European Aerosol Research Lidar Network
IAVW	International Airways Volcano Watch
RH	Relative Humidity
UTLS	Upper Troposphere - Lower Stratosphere
VATD	Volcanic Ash Transport and Dispersal

References

- Ansmann, A., et al., Ash and fine-mode particle mass profiles from earlinet-aeronet observations over central europe after the eruptions of the eyjafjallajökull volcano in 2010, *Journal of Geophysical Research: Atmospheres*, 116(D20), doi:10.1029/2010JD015567, 2011.
- Barr, S., Skirt clouds associated with the soufriere eruption of 17 april 1979, *Science*, 216(4550), 1111–1112, 1982.
- Bear-Crozier, A., S. Pouget, M. Bursik, E. Jansons, J. Denman, A. Tupper, and R. Rustowicz, Automated detection and measurement of volcanic cloud growth: towards a robust estimate of mass flux, mass loading and eruption duration, *Natural Hazards*, pp. 1–38, 2020.
- Britter, R. E., and J. E. Simpson, A note on the structure of the head of an intrusive gravity current, *Journal of Fluid Mechanics*, 112, 459–466, doi:10.1017/S0022112081000517, 1981.
- Bursik, M., Tephra dispersal, in *The Physics of Explosive Volcanic Eruptions, Special Publications*, vol. 145, edited by J. S. Gilbert and R. S. J. Sparks, pp. 117–146, Geological Society of London, illus. incl. sketch maps, 1998.
- Carazzo, G., and A. M. Jellinek, A new view of the dynamics, stability and longevity of volcanic clouds, *Earth and Planetary Science Letters*, 325, 39–51, 2012.
- Carazzo, G., and A. M. Jellinek, Particle sedimentation and diffusive convection in volcanic ash-clouds, *Journal of Geophysical Research*, 118, 1420–1437, 2013.
- Casadevall, T. J., Volcanic ash and aviation safety: Proceedings of the first international symposium on volcanic ash and aviation safety, *U.S. Geological Survey Bulletin*, 2047, 450, 1994.

- Chakraborty, P., G. Gioia, and S. Kieffer, Volcán reventador’s unusual umbrella, *Geophysical research letters*, 33(5), 2006.
- Cho, J. Y., R. E. Newell, B. E. Anderson, J. D. Barrick, and K. L. Thornhill, Characterizations of tropospheric turbulence and stability layers from aircraft observations, *Journal of Geophysical Research: Atmospheres*, 108(D20), 2003.
- Clayson, C. A., and L. Kantha, On turbulence and mixing in the free atmosphere inferred from high-resolution soundings, *Journal of Atmospheric and Oceanic Technology*, 25(6), 833–852, 2008.
- Csanady, D. T., Turbulent diffusion in the environment, *D.Reidel Publishing Co*, p. 248p, dordrecht, 1980.
- Dacre, H., A. Grant, N. Harvey, D. Thomson, H. Webster, and F. Marengo, Volcanic ash layer depth: Processes and mechanisms, *Geophysical Research Letters*, 42(2), 637–645, 2015.
- Dehghan, A., W. K. Hocking, and R. Srinivasan, Comparisons between multiple in-situ aircraft turbulence measurements and radar in the troposphere, *Journal of Atmospheric and Solar-Terrestrial Physics*, 118, 64–77, 2014.
- Devenish, B., D. Thomson, F. Marengo, S. Leadbetter, H. Ricketts, and H. Dacre, A study of the arrival over the united kingdom in april 2010 of the eyjafjallajökull ash cloud using ground-based lidar and numerical simulations, *Atmospheric Environment*, 48, 152 – 164, doi:<https://doi.org/10.1016/j.atmosenv.2011.06.033>, volcanic ash over Europe during the eruption of Eyjafjallajökull on Iceland, April-May 2010, 2012.
- Fero, J., S. N. Carey, and J. T. Merrill, Simulating the dispersal of tephra from the 1991 pinatubo eruption: implications for the formation of widespread ash layers, *Journal of Volcanology and Geothermal Research*, 186(1-2), 120–131, 2009.
- Folch, A., A. Costa, and S. Basart, Validation of the fall3d ash dispersion model using observations of the 2010 eyjafjallajökull volcanic ash clouds, *Atmospheric Environment*, 48, 165 – 183, doi:<https://doi.org/10.1016/j.atmosenv.2011.06.072>, volcanic ash over Europe during the eruption of Eyjafjallajökull on Iceland, April-May 2010, 2012.
- Gage, K., J. Green, and T. VanZandt, Use of doppler radar for the measurement of atmospheric turbulence parameters from the intensity of clear-air echoes, *Radio Science*, 15(2), 407–416, 1980.
- Heinold, B., I. Tegen, R. Wolke, A. Ansmann, I. Mattis, A. Minikin, U. Schumann, and B. Weinzierl, Simulations of the 2010 eyjafjallajökull volcanic ash dispersal over europe using cosmo–muscat, *Atmospheric Environment*, 48, 195 – 204, doi: <https://doi.org/10.1016/j.atmosenv.2011.05.021>, volcanic ash over Europe during the eruption of Eyjafjallajökull on Iceland, April-May 2010, 2012.
- Holasek, R. E., S. Self, and A. W. Woods, Satellite observations and interpretation of the 1991 mount pinatubo eruption plumes, *Journal of Geophysical Research*, 12(27), 635–27, 1996a.

- Holasek, R. E., A. W. Woods, and S. Self, Experiments on gas-ash separation processes in volcanic umbrella clouds, *Journal of Volcanology Geothermal Research*, *70*, 169–181, 1996b.
- Hopkins, A. T., and C. J. Bridgman, A volcanic ash transport model and analysis of mount st. helens ashfall, *Journal of Geophysical Research*, *90*, 10,620–10,630, 1985.
- Hoyal, D. C. J. D., M. I. Bursik, and J. F. Atkinson, Setting-driven convection; a mechanism of sedimentation from stratified fluids, *Journal of Geophysical Research, C, Oceans*, *104*(4), 7953–7966, illus. incl. 1 table, 1999a.
- Hoyal, D. C. J. D., M. I. Bursik, and J. F. Atkinson, The influence of diffusive convection on sedimentation from buoyant plumes, *Marine Geology*, *159*(1-4), 205–220, 1999b.
- Jonsson, H. H., J. C. Wilson, C. A. Brock, J. E. Dye, G. V. Ferry, and K. R. Chan, Evolution of the stratospheric aerosol in the northern hemisphere following the june 1991 volcanic eruption of mount pinatubo: Role of tropospheric-stratospheric exchange and transport, *Journal of Geophysical Research*, *101*, 1553–1570, 1996.
- Kristiansen, N. I., A. Prata, A. Stohl, and S. A. Carn, Stratospheric volcanic ash emissions from the 13 february 2014 kelut eruption, *Geophysical Research Letters*, *42*(2), 588–596, 2015.
- Madankan, R., et al., Computation of probabilistic hazard maps and source parameter estimation for volcanic ash transport and dispersion, *Journal of Computational Physics*, *271*(0), 39 – 59, doi:http://dx.doi.org/10.1016/j.jcp.2013.11.032, frontiers in Computational Physics Modeling the Earth System, 2014.
- Maekawa, Y., S. Fukao, M. Yamamoto, M. D. Yamanaka, T. Tsuda, S. Kato, and R. F. Woodman, First observation of the upper stratospheric vertical wind velocities using the jicamarca vhf radar, *Geophysical research letters*, *20*(20), 2235–2238, 1993.
- Marenco, F., B. Johnson, K. Turnbull, S. Newman, J. Haywood, H. Webster, and H. Ricketts, Airborne lidar observations of the 2010 eyjafjallajökull volcanic ash plume, *Journal of Geophysical Research: Atmospheres*, *116*(D20), 2011.
- Mazzocchi, M., F. Hansstein, and M. Ragona, The 2010 volcanic ash cloud and its financial impact on the european airline industry, in *CESifo Forum*, vol. 11, pp. 92–100, München: ifo Institut für Wirtschaftsforschung an der Universität München, 2010.
- Pavelin, E., J. A. Whiteway, R. Busen, and J. Hacker, Airborne observations of turbulence, mixing, and gravity waves in the tropopause region, *Journal of Geophysical Research: Atmospheres*, *107*(D10), ACL–8, 2002.
- Pavolonis, M. J., A. K. Heidinger, and J. Sieglaff, Automated retrievals of volcanic ash and dust cloud properties from upwelling infrared measurements, *Journal of Geophysical Research: Atmospheres*, *118*(3), 1436–1458, doi:10.1002/jgrd.50173, 2013.

- Pierce, R. B., and T. D. A. Fairlie, Chaotic advection in the stratosphere: Implications for the dispersal of chemically perturbed air from the polar vortex, *Journal of Geophysical Research: Atmospheres*, 98(D10), 18,589–18,595, 1993.
- Pouget, S., M. Bursik, P. Webley, J. Dehn, and M. Pavolonis, Estimation of eruption source parameters from umbrella cloud or downwind plume growth rate, *Journal of Volcanology and Geothermal Research*, 258, 100–112, 2013.
- Pouget, S., M. Bursik, C. G. Johnson, A. J. Hogg, J. C. Phillips, and R. S. J. Sparks, Interpretation of umbrella cloud growth and morphology: implications for flow regimes of short-lived and long-lived eruptions, *Bulletin of Volcanology*, 78(1), 1–19, doi:10.1007/s00445-015-0993-0, 2016.
- Prata, F., M. Woodhouse, H. E. Huppert, A. Prata, T. Thordarson, and S. Carn, Atmospheric processes affecting the separation of volcanic ash and so₂ in volcanic eruptions: inferences from the may 2011 grímsvötn eruption, *Atmospheric Chemistry and Physics*, 17(17), 10,709–10,732, 2017.
- Roberts, P. J., and D. R. Webster, Turbulent diffusion, in *Environmental Fluid Mechanics: Theories and Applications*, edited by H. H. Shen, A. H. Cheng, K.-H. Wang, M. H. Teng, and C. C. Liu, pp. 7–45, ASCE Press, Reston, Virginia, 2002.
- Schumann, U., et al., Airborne observations of the eyjafjalla volcano ash cloud over europe during air space closure in april and may 2010, *Atmos. Chem. Phys.*, 11, 2245–2279, doi:10.5194/acp-11-2245-2011, 2011.
- Schwaiger, H. F., R. P. Denlinger, and L. G. Mastin, Ash3d: A finite-volume, conservative numerical model for ash transport and tephra deposition, *Journal of Geophysical Research: Solid Earth*, 117(B4), 2012.
- Scollo, S., M. Coltelli, F. Prodi, M. Folegani, and S. Natali, Terminal settling velocity measurements of volcanic ash during the 2002–2003 etna eruption by an x-band microwave rain gauge disdrometer, *Geophysical Research Letters*, 32(10), 2005.
- Sharman, R. D., S. B. Trier, T. P. Lane, and J. D. Doyle, Sources and dynamics of turbulence in the upper troposphere and lower stratosphere: A review, *Geophys Res Lett*, 39, doi:10.1029/2012GL051996, 2012.
- Sparks, R. S. J., M. I. Bursik, S. N. Carey, J. S. Gilbert, L. S. Glaze, H. Sigurdsson, and A. W. Woods, *Volcanic Plumes*, John Wiley & Sons, London, 574p., 1997.
- Thorsteinsson, T., T. Jóhannsson, A. Stohl, and N. I. Kristiansen, High levels of particulate matter in iceland due to direct ash emissions by the eyjafjalla-jökull eruption and resuspension of deposited ash, *Journal of Geophysical Research: Solid Earth*, 117(B9), 2012.
- Thouret, V., J. Y. Cho, R. E. Newell, A. Marenco, and H. G. Smit, General characteristics of tropospheric trace constituent layers observed in the mozaic program, *Journal of Geophysical Research: Atmospheres*, 105(D13), 17,379–17,392, 2000.

- Tupper, A., S. Carn, J. Davey, Y. Kamada, R. Potts, F. Prata, and M. Tokuno, An evaluation of volcanic cloud detection techniques during recent significant eruptions in the western 'ring of fire', *Remote Sensing of Environment*, 91(1), 27–46, 2004.
- Tupper, A., I. Itikarai, M. Richards, F. Prata, S. Carn, and D. Rosenfeld, Facing the challenges of the international airways volcano watch: the 2004/05 eruptions of manam, papua new guinea, *Weather and Forecasting*, 22(1), 175–191, 2007.
- Tupper, A., C. Textor, M. Herzog, and H.-F. Graf, Tall clouds from small eruptions: modelling the sensitivity of eruption height and fine ash fallout to tropospheric instability, *Natural Hazards*, doi:10.1007/s11069-009-9433-9, 2009.
- Vasseur, H., and D. Vanhoenacker, Characteristics of tropospheric turbulent layers from radiosonde data, *Electronic Letters*, 34, 318–319, 1998.
- Vernier, J.-P., et al., An advanced system to monitor the 3d structure of diffuse volcanic ash clouds, *Journal of applied meteorology and climatology*, 52(9), 2125–2138, 2013.
- Wilson, R., Turbulent diffusivity in the free atmosphere inferred from mst radar measurements: a review, *Annales Geophysicae*, 22, 3869–3887, 2004.
- Wilson, R., H. Luce, H. Hashiguchi, N. Nishi, and Y. Yabuki, Energetics of persistent turbulent layers underneath mid-level clouds estimated from concurrent radar and radiosonde data, *Journal of Atmospheric and Solar-Terrestrial Physics*, 118, 78–89, 2014.
- Winker, D., and M. Osborn, Preliminary analysis of observations of the pinatubo volcanic plume with a polarization-sensitive lidar, *Geophysical research letters*, 19(2), 171–174, 1992.
- Winker, D., Z. Liu, A. Omar, J. Tackett, and D. Fairlie, Caliop observations of the transport of ash from the eyjafjallajökull volcano in april 2010, *Journal of Geophysical Research: Atmospheres*, 117(D20), 2012.
- Woods, A. W., and J. Kienle, The dynamics and thermodynamics of volcanic clouds: Theory and observations from the april 15 and april 21, 1990 eruptions of redoubt volcano, alaska, *Journal of Volcanology and Geothermal Research*, 62(1-4), 273–299, 1994.
- Wright, S. J., Effects of ambient crossflows and density stratification on the characteristic behavior of round turbulent buoyant jets, *W.M. Keck Laboratory, Caltech, Pasadena, Report KH-R-36*, 1977.